JOURNAL OF BACTERIOLOGY, Sept. 2001, p. 5102–5109 Vol. 183, No. 17
0021-9193/01/$04.00+0 DOI: 10.1128/JB.183.17.5102–5109.2001
Copyright © 2001, American Society for Microbiology. All Rights Reserved.

Insertional Mutagenesis in the *n*-Alkane-Assimilating Yeast *Yarrowia lipolytica*: Generation of Tagged Mutations in Genes Involved in Hydrophobic Substrate Utilization

STEPHAN MAUERSBERGER,[1] HUI-JIE WANG,[2] CLAUDE GAILLARDIN,[2] GEROLD BARTH,[1] AND JEAN-MARC NICAUD[2]*

Laboratoire de Microbiologie et de Génétique Moléculaire, UR INRA 216, URA CNRS 1925, Institut National Agronomique Paris-Grignon, F-78850 Thiverval-Grignon, France,[2] and Institut für Mikrobiologie, Technische Universität Dresden, D-01062 Dresden, Germany[1]

Received 22 March 2001/Accepted 13 June 2001

Tagged mutants affected in the degradation of hydrophobic compounds (HC) were generated by insertion of a *zeta-URA3* mutagenesis cassette (MTC) into the genome of a *zeta*-free and *ura3* deletion-containing strain of *Yarrowia lipolytica*. MTC integration occurred predominantly at random by nonhomologous recombination. A total of 8,600 Ura^+ transformants were tested by replica plating for (i) growth on minimal media with alkanes of different chain lengths (decane, dodecane, and hexadecane), oleic acid, tributyrin, or ethanol as the C source and (ii) colonial defects on different glucose-containing media (YPD, YNBD, and YNBcas). A total of 257 mutants were obtained, of which about 70 were affected in HC degradation, representing different types of non-alkane-utilizing (Alk^-) mutants (phenotypic classes alkA to alkE) and tributyrin degradation mutants. Among Alk^- mutants, growth defects depending on the alkane chain length were observed (alkAa to alkAc). Furthermore, mutants defective in yeast-hypha transition and ethanol utilization and selected auxotrophic mutants were isolated. Flanking borders of the integrated MTC were sequenced to identify the disrupted genes. Sequence analysis indicated that the MTC was integrated in the *LEU1* locus in N083, a leucine-auxotrophic mutant, in the isocitrate dehydrogenase gene of N156 (alkE leaky), in the thioredoxin reductase gene in N040 (alkAc), and in a peroxine gene (*PEX14*) in N078 (alkD). This indicates that MTC integration is a powerful tool for generating and analyzing tagged mutants in *Y. lipolytica*.

About 20% of all yeast species have been recorded as being able to utilize as carbon substrates hydrophobic compounds (HC) like *n*-alkanes, fatty acids, and triglycerides (for reviews see references 15 and 36). This list of species was significantly extended by studies on single-cell protein production in the mid-1960s (30). Among these yeasts, however, genetic and genetic-engineering techniques were widely developed only for the dimorphic fungus *Yarrowia* (formerly *Candida*, *Endomycopsis*, or *Saccharomycopsis*) *lipolytica* (2).

Y. lipolytica very efficiently utilizes long- and short-chain triglycerides, such as olive oil and tributyrin, fatty acids, and the corresponding *n*-alkanes, from decane (C_{10}) to octadecane (C_{18}) and longer chains (2). Screening of mutants affected in HC utilization was initially performed by R. K. Mortimer's group (5) using *n*-decane as the substrate. Based on the relative frequencies of alkane and auxotrophic mutants, 80 to 90 genes appeared to be involved in *n*-alkane assimilation. The Alk^- mutants were classified into five phenotypic classes (alkA to alkE) depending on their use of intermediates of the alkane degradation pathway (fatty alcohol, fatty aldehyde, fatty acid, and acetate) (5, 6, 14, 17). Among at least 26 loci affecting uptake and primary alkane oxidation, 16 were required for efficient *n*-alkane uptake (6). Mauersberger et al. isolated Alk^- mutants of *Y. lipolytica* and *Candida maltosa* using C_{10}, C_{12}, and C_{16} as substrates and subdivided alkA mutants into alkAa (unable to use any *n*-alkane), alkAb (no growth on C_8 to C_{10}), and alkAc (no growth on C_{16}) (17). This, and studies on cytochrome P450 regulation in *Y. lipolytica* and *C. maltosa*, suggested the existence of several chain length-specific alkane uptake or cytochrome P450 monooxygenase systems catalyzing the primary terminal hydroxylation (17). This was proven for *C. maltosa* (23, 37) and more recently for *Y. lipolytica* (12), by identifying up to eight cytochrome P450 genes (*ALK1* to *ALK8*) in this species, all belonging to the *CYP52* gene family. A *Y. lipolytica* strain with *ALK1* deleted grew very poorly on C_{10} but almost normally on C_{12} or C_{16} (11).

Other groups isolated mutants unable to utilize short-chain triglycerides after nystatin enrichment using tributyrin as a carbon source (19, 20) or unable to utilize the long-chain oleic acid (C_{18}) in a screen of genes involved in peroxisome biogenesis using a rapid immunofluorescence assay (22). Some of the Pex mutants exhibited pleiotropic phenotypes affecting peroxisome biogenesis, secretion, and morphology (32). Several *PEX* genes were isolated, and their functions were analyzed (32, 33).

Through both reverse and classical genetics, we identified multigene families involved in these metabolic pathways, such as those encoding acyl-coenzyme A oxidases of the peroxisomal β-oxidation (*POX1* to *POX5* genes) (35) or lipases (*LIP* genes) (24), and genes impairing the anaplerotic glyoxylate cycle and its regulation during metabolism of alkanes, ethanol, or acetate (*ICL1*, *ACS1*, and *GPR1*) (4, 14, 34).

* Corresponding author. Mailing address: Laboratoire de Microbiologie et de Génétique Moléculaire, Institut National Agronomique Paris-Grignon, BP 01, F-78850 Thiverval-Grignon, France. Phone: 33 01 30 81 54 50. Fax: 33 01 30 81 54 57. E-mail: jean-marc.nicaud@grignon.inra.fr.

TABLE 1. *Y. lipolytica* strains used in this study

Name	Genotype	References
W29	*MATA*, wild-type	3
PO1d	*MATA leu2-270 ura3-302 xpr2-322 SUC2*	3
E129	*MATA leu2-270 lys11-23 ura3-302 xpr2-322 SUC2*	3
E150	*MATB leu2-270 his1 ura3-302 xpr2-322 SUC2*	3
YB423-12	*MATA*, wild-type	3
CX161-1B	*MATA ade1*	5
CXAU1	*MATA ade1, ura3*	11
H222	*MATA*, wild-type	3
H222-67	*MATA ura3-67*	16
H222-41 (JMY322)	*MATA ura3-41*	This work
H222-S4 (JMY323)	*MATA ura3-302 SUC2*	This work
B204-12C-20	*MATA leu2-20 met6-1 spo1-1*	14
B204-67 (JMY324)	*MATA leu2-20 met6-1 spo1-1 ura3-674*	This work
T1 to T20	H222-41 transformed with JMP5 digested by *Not*I, randomly selected Ura$^+$	
P1 to P20	H222-41 transformed with JMP5 digested by *Not*I, with phenotype	
N001 to N257	H222-41 transformed with JMP5 digested by *Not*I with selected phenotypes	

Several of the previously isolated Alk$^-$ mutants were simultaneously affected in mating and/or sporulation, in colonial and cellular morphology, and/or in transformation ability (5, 6). In addition, for several chemically induced alkE mutants, revertants with new phenotypes occurred at high frequencies (16). To circumvent these difficulties, we first developed a transposon tagging approach to identify genes involved in HC utilization (18), leading to the characterization of *PEX10* (J.-M. Nicaud, unpublished data), which is involved in peroxisome biogenesis. However, identification of the tagged genes was plagued by a high level of nonhomologous integration (26).

We recently developed new integrative vectors (mono- and multicopy) for gene expression in *Y. lipolytica* (25), carrying the *zeta* long terminal repeat of the *Y. lipolytica* retrotransposon *Ylt1* (29). We observed that this long terminal repeat directed random integration of the transforming DNA into the genome of strains devoid of *Ylt1*. Here, we report on the use of a short *zeta*-based mutagenesis cassette (MTC) for generating tagged mutants. We demonstrate that this MTC inserts at random by nonhomologous recombination, that mutant phenotypes are due to cassette integration, and that tagged genes are easily identified. This provides a powerful tool for the identification of genes involved in different pathways, as demonstrated here for HC utilization, morphogenesis, and auxotrophic mutants.

MATERIALS AND METHODS

Strains, media, and growth conditions. The *Escherichia coli* DH5α strain was used for transformation and amplification of recombinant plasmids DNA. Cells were grown in Luria-Bertani medium (27) supplemented with ampicillin (100 μg/ml) or kanamycin (40 μg/ml) for plasmid selection. The *Y. lipolytica* strains used in this study are listed in Table 1. They were grown at 28°C in complete media, YPD (3), and YNBcas (YNBD with 0.2% Casamino Acids) (35) or in minimal media derived from YNB (35) or M (a slightly modified YNB medium) (17) containing the following carbon sources: glucose (1 or 2%; YNBD), oleic acid (1% in 0.05% Tween 80, added as 20-fold sonicated stock emulsion; YNBO), tributyrin (1% in 0.05% Tween 80, added as 20-fold sonicated emulsion; YNBT), alkanes (1 or 2%) of different chain lengths (YNBC10, decane; YNBC12, dodecane; YNBC16, hexadecane). For solid media, 20 g of agar per liter was added. For alkane growth test on plates, alkanes were supplied as vapor phase by placing 200 μl of the *n*-alkane on a sterile filter paper in the lid of the petri dish (16, 17). Amino acids and uracil were supplied when necessary.

Cultivation in liquid media was performed with 100 or 200 ml of minimal YNB or M medium in 500-ml Erlenmeyer shaking flasks; baffled flasks were used to improve dispersion of alkanes and oxygen supply. Cells from overnight YPD cultures were centrifuged, washed twice with minimal medium without a carbon source, and used to inoculate the culture at an initial optical density at 600 nm (OD_{600}) of 0.4 to 0.6. Growth was followed by measuring the OD_{600} or alkali (2.5 N NaOH) consumption used for maintaining pH at 5.3 to 5.5 in minimal medium (10).

Plasmid constructions. All basic DNA manipulation procedures were performed according to reference 27. The construction of plasmids JMP5 (Fig. 1) and pINA302 was described previously (21, 25); the construction of pCR4 is described below.

Sequencing of the URA3 locus, construction of pCR4, and isolation of strains carrying nonreverting *ura3* alleles. To increase the upstream and downstream sequence information about the *URA3* gene locus (U40564), we sequenced over 4,844 bp for this locus (AJ306421) by primer walking using plasmid pLD55, containing a 4.6-kb *Sau*3A *Y. lipolytica* DNA insert (obtained from L. S. Davidow, Pfizer Inc. [8a]), and plasmid AWOAA010FO3, from a library of 2,284 plasmids used for generating 4,940 random sequence tags (RSTs) from strain W29 (8).

URA3 deletions in the recipient strains were constructed by transformation using either pINA302 (containing a *ura3*::*SUC2* construct [21]) or a new *URA3* disruption plasmid, pCR4, containing larger flanking regions. Plasmid pCR4 was constructed by PCR amplification of *URA3* promoter (620 bp) and terminator

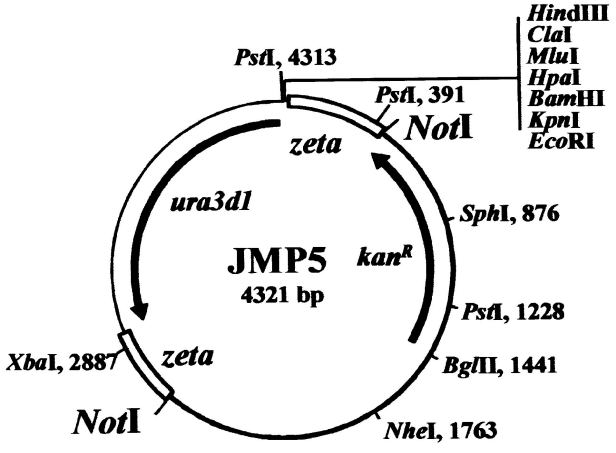

FIG. 1. Schematic map of plasmid JMP5. For insertion mutagenesis, plasmid JMP5 (35) was digested by *Not*I prior transformation to eliminate the bacterial pHSS6 region (thick line) and to liberate the MTC containing only the nondefective *Y. lipolytica ura3d1* allele (arrow), flanked by two inverted partial *zeta* regions of 401 and 312 bp (open boxes). The gene conferring kanamycin resistance (*kan^R*) in *E. coli* is also shown by an arrow.

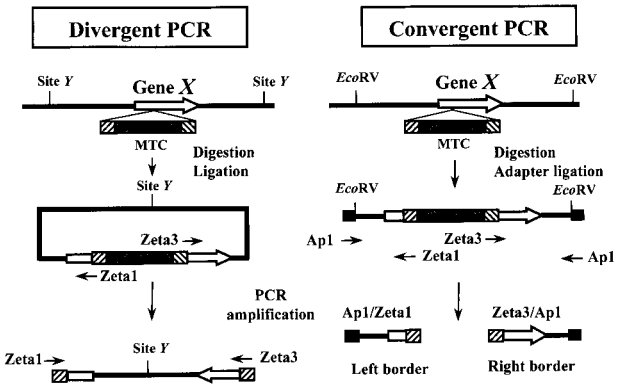

FIG. 2. Strategies for sequencing of the *zeta-URA3* MTC insertion sites in the tagged mutants. Divergent and convergent PCR methods were used for amplification of the MTC (grey box, *ura3d1*; flanking hatched boxes, *zeta* fragments) insertion site borders. (Left) Divergent PCR method to rescue the genomic sequences flanking the MTC inserted into gene X (white arrows, borders after insertion). Genomic DNA (black line) of MTC mutants was digested with an enzyme which does not cut in the MTC (site Y) and circularized by ligation. PCR amplification was performed with oligonucleotide primers (thin arrows) specific for the MTC (Zeta1 and Zeta3). Alternatively, a restriction enzyme was used that cuts in the polylinker of the MTC (Fig. 1, *Hin*dIII to *Eco*RI), followed by amplification of the left and right borders as described previously for Tn*3* insertion in *Y. lipolytica* (26). The PCR product was sequenced using the same primers. (Right) Convergent PCR method (PCR walking). Genomic DNA of selected MTC mutants was digested with enzymes giving blunt ends, such as *Eco*RV or *Eco*RV plus *Stu*I plus *Pvu*II), and ligated with the specific adapter oligonucleotides Ad1 and Ad2 (black boxes) as previously described (9). PCR was performed with a primer specific to the adapter (Ap1) and with a primer specific to the MTC, like Zeta1 and Zeta3, generating left and right border fragments, respectively. Border fragments were sequenced with the same primers.

regions (2.6 kb) from plasmid pLD55 and ligation as *Hin*dIII/blunt-end and blunt-end/*Sst*I fragments into pUC18. It contains a nearly complete deletion (bp 1206 to 2019) of the *URA3* open reading frame (bp 1195 to 2049). After transformation of strains H222, B204-12C, and B204-12C-20 with plasmid pCR4 (digested with *Hin*dIII and *Sst*I) and subsequent 5-fluoroorotic acid selection, we isolated several stable Ura$^-$ strains. Southern blotting and PCR analysis of 15 Ura$^-$ clones from each strain revealed that several harbored *URA3* deletions, but never of the expected type. The *URA3* deletions were mapped by sequencing after PCR amplification using the primer pair URA3-dis1 (GGGGTGACACT GCACTATTGGTTTG) and URA3-dis2 (CATGTACTCTGCCTCTCAG AAC GC). The coordinates, corresponding to the known 4,844-bp sequence (AJ306421) of the *Y. lipolytica URA3* locus are bp 1195 to 2049 for the *URA3* open reading frame, bp 1804 to 1814 for a *ura3-41* 10-bp deletion in strain H222-41, bp 1211 to 2152 for the *ura3-302* deletion in strain H222-S4, and bp 1167 to 3385 for the *ura3-67* deletion in strain B204-67.

Transformation of *Y. lipolytica*. Transformation was performed by the lithium acetate method as previously described (3). Plasmid JMP5 (Fig. 1) was digested by *Not*I prior to transformation. For each transformation assay, 0.5 to 1 μg of plasmid DNA was used, yielding about 1,000 to 1,500 transformants per μg of DNA. Ura$^+$ transformants were selected on YNBcas.

Chromosomal DNA preparation and Southern blot analysis. Genomic DNA was prepared as described previously (3). Probes were prepared by PCR or as DNA fragments from plasmids and labeled with the Gene Images random prime labeling and detection system (Amersham Life Science).

Amplification of the MTC borders and sequences analysis. The MTC borders were amplified either by divergent PCR (Fig. 2) as described previously (26) or by convergent PCR walking (31) (Fig. 2). Primers Ad1, Ad2, and Ap1 are described in references 9 and 31, and the MTC-specific primers are Zeta1 (CCCCACTATGAATACATCAG) and Zeta3 (CACTACCGAGGTTACTAG AG). For PCR walking or convergent PCR (Fig. 2), left and right borders were amplified with the primer pairs Ap1-Zeta1 and Ap1-Zeta3, respectively. All amplifications were performed on a Perkin-Elmer thermal cycler 2400 with the Expand long-template PCR system (Roche Diagnostics GmbH) as previously described (26). PCR fragments were sequenced directly after gel purification on an ABI373 DNA sequencer according to the manufacturer's instructions (Perkin-Elmer Biosystems). Sequence comparisons were done by BLAST search (1) against a *Y. lipolytica* RST database (8) and at http://www.ncbi.nlm.nih.gov/blast /blast.cgi. The *LEU1* gene was amplified with primers N083-1 (TCAAGGACT TTGGCGTG) and N083-2 (GAAAAAGAGACCCGAGG).

Nucleotide sequence accession numbers. DNA sequences were deposited in the EMBL database under the accession numbers AJ306421 for *URA3* and AJ278693 for *LEU1*.

RESULTS AND DISCUSSION

Choice and construction of recipient strains. Natural isolates of *Y. lipolytica* appear to have widely divergent genetic structures, as indicated by chromosome length polymorphism (7) and by the presence or absence of the retrotransposon *Ylt1* (8). For this study, we required a strain that (i) was devoid of *Ylt1* in order to obtain dispersed integration of a *zeta-URA3* cassette, (ii) grew efficiently on hydrophobic substrates, and (iii) exhibited a clear dimorphic switch. We therefore tested for

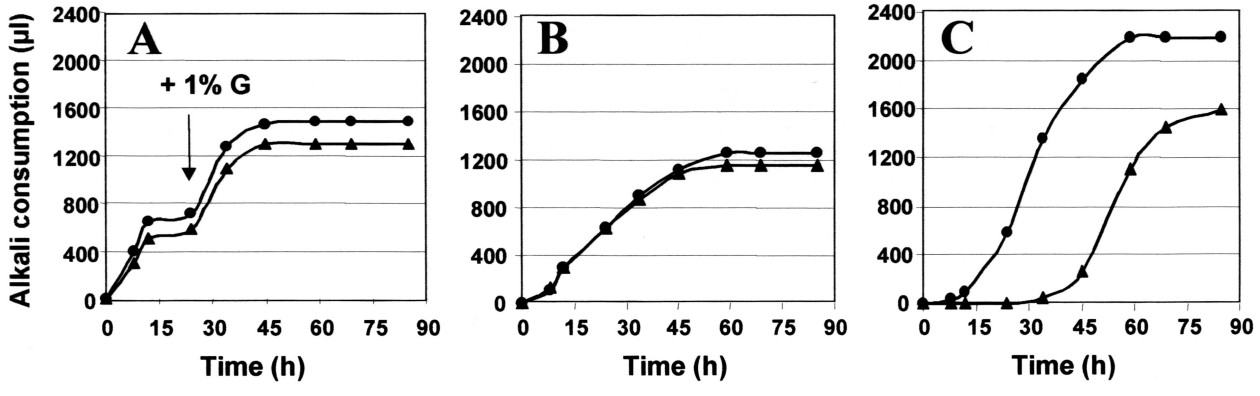

FIG. 3. Growth comparison of *Y. lipolytica* wild-type strains. Growth of the strains H222 (●) and W29 (▲) in minimal medium M with 1% glucose (arrow, additional 1% glucose supplied at 24 h) (A), 1% oleic acid (B), and 2% hexadecane (baffled shaking flasks) (C) as carbon sources. Cultures in 100 ml of M medium in 500-ml shaking flasks were inoculated with washed cells from overnight YPD precultures at 2×10^6 cells/ml (OD_{600} = 0.4). Growth was monitored by measuring the amount of alkali (2.5 N NaOH) consumption used for pH titration to 5.5 as described previously (10).

the presence of *Ylt1* in various strains, like the wild-type strain YB423, its derivatives CX161-1B and CXAU1 (American strain series), or the wild-type strain H222 from Germany, all previously used for isolation of non-alkane-utilizing (Alk^-) mutants (5, 6, 16) and cytochrome P450 studies (11, 12). We also tested inbred German strains of G. Barth's laboratory, such as B204-12C and its derivatives, inbred French strains such as E129 and E150, used for the isolation of peroxisomal mutants (22), and the French wild-type strain W29, used in the recent *Y. lipolytica* sequencing projects (8). The American strains and all inbred strains derived from them contain the *Ylt1* retrotransposon, while the French (W29) and German (H222) wild-type strains were devoid of it (data not shown; see also reference 13).

Both W29 and H222 exhibit similar morphology and growth kinetics on the various media tested, except for *n*-alkanes, where W29 exhibits a very long lag phase or no growth at all when replica plated from a glucose to an alkane medium. Similar growth kinetics are observed in liquid medium on glucose (Fig. 3A) and oleic acid (Fig. 3B), while W29 exhibits a 30- to 35-h lag phase on alkanes of different chain lengths (C_{10} to C_{16}), as shown for hexadecane (Fig. 3C).

In addition, we observed that amino acid-auxotrophic strains (Leu^-, Met^-, Lys^-, or His^-) exhibited a reduced growth rate in minimal medium on HC, but also on glucose, glycerol, or ethanol, when ammonium salts were given as nitrogen source (35; T. Juretzek and S. Mauersberger, unpublished results). Thus, only a *ura3* derivative of the wild-type strain H222 exhibited the required characteristics for this study.

Existing UV-induced mutants like H222-67 (*ura3-67*) were found to revert at too high a frequency for tagged mutagenesis. We therefore constructed H222 derivatives with nonreverting *ura3* alleles (see Materials and Methods).

We used here strain H222-41, which contains a nonreverting 10-bp deletion (allele *ura3-41*), although strains with larger deletions obtained later (see Materials and Methods) might be less prone to *URA3* conversion events during transformation (see below).

Isolation of tagged mutants with a *zeta-URA3* MTC. During analysis of *Y. lipolytica* Tn*3*-tagged mutants (18), we frequently observed unexpected events such as nonhomologous recombination, which complicated identification of the insertion site (26; J.-M. Nicaud et al., unpublished data).

We therefore wanted to test if a simpler MTC, containing only a selectable marker flanked by *zeta* regions for promoting random integration into the genome of *Ylt1*-free strains, could be used to tag *Y. lipolytica* genes. For this purpose the strain *Y. lipolytica* H222-41 (*ura3-41*) was transformed with *Not*I-digested JMP5 (Fig. 1), thus liberating the MTC from the vector. Ura^+ transformant colonies were selected on YNBcas at a frequency of 1,000 to 1,500 transformants per μg of DNA. A total of approximately 8,600 transformants were isolated and tested for phenotypes (see below).

The integration of the MTC into the genome was studied by Southern blot analysis of 20 randomly selected Ura^+ transformants (T clones) (Fig. 4B) and of 21 Ura^+ transformants exhibiting specific phenotypes (P clones) (Fig. 4C). When genomic DNA was digested by *Eco*RV and hybridized with a *URA3* probe, several bands were expected (Fig. 4A). For the genomic *ura3-41* locus, three bands of 5.6 kb (band a), 2,507 bp

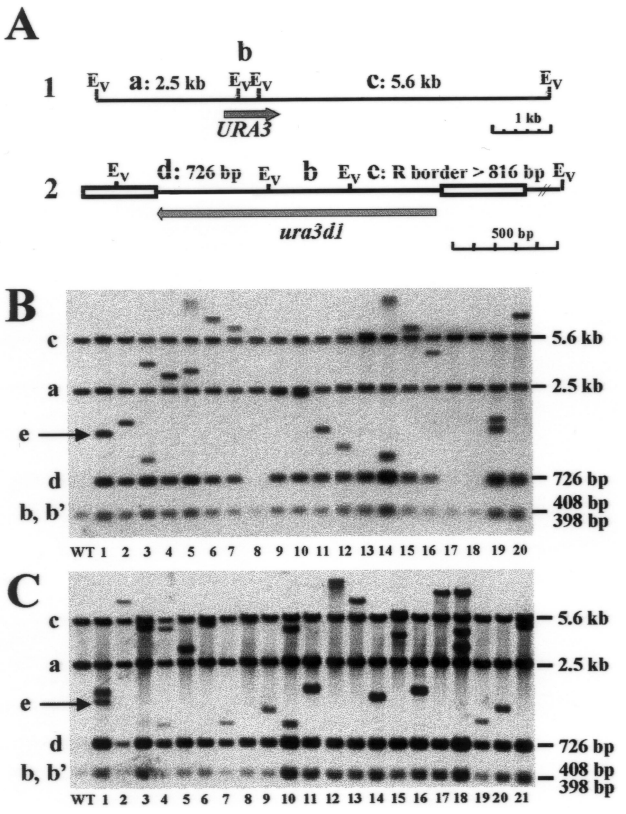

FIG. 4. Southern blot analysis of MTC transformants revealing random cassette integration. (A) Schematic representation of the genomic *URA3* locus (construct 1) and of a locus where a *zeta-URA3* MTC was inserted (construct 2). The expected fragments (a to e) and their sizes are indicated. Abbreviations: Ev, *Eco*RV; R, right. (B) MTC integration into the genome was determined by Southern blot analysis of 20 randomly selected Ura^+ transformants (T clones) of strain H222-41 with the MTC. Genomic DNA of the wild-type strain H222 (lane WT) and 20 T clones (lanes 1 to 20) from one transformation plate was digested with *Eco*RV and probed with the entire *URA3* open reading frame. (C) Southern blot hybridization of 21 selected transformants of strain H222-41 with the MTC, showing phenotypes in the first screen (P clones, lanes 1 to 21) and of the wild-type strain H222 (WT). Conditions were as described for panel B. (B and C) Band names and sizes correspond to those in panel A. The variable right border (band e) is indicated by an arrow for the first transformants, T1 (B) and P1 (C).

(band b), and 398 bp (band c) were expected, the latter being replaced by a 408-bp band in the case of the wild-type locus or of the *ura3d1* allele (Fig. 4A, construct 1). This was indeed observed in strain H222 and in all transformants (Fig. 4B and C, lanes 1, 2 to 20, and 2 to 21, respectively). When the MTC inserted randomly into genomic DNA, three bands were predicted: a new 726-bp band (band d), an internal 408-bp fragment (band b), and one larger than 816 bp and reflecting the location of the closest genomic *Eco*RV site in the right border (band e) (Fig. 4A, construct 2).

In the transformants (Fig. 4B and C), three types of patterns could be observed. A wild-type pattern (type I, bands a, b, and c), identical to that of strain H222, was observed for the randomly selected T clones 8, 17, and 18 (Fig. 4B and C, lanes 1), reflecting *ura3-41* conversion in 15% of the transformants. No type I event was observed among P clones (Fig. 4C). The

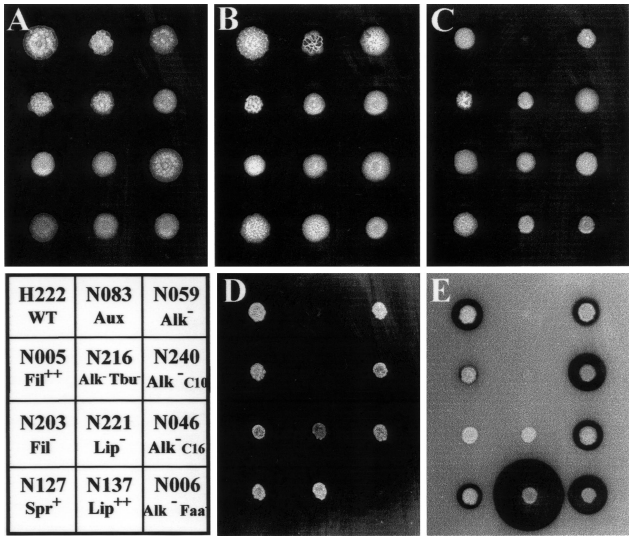

FIG. 5. Phenotypes of selected *zeta-URA3* MTC insertion mutants. Wild-type strain H222 (WT) and selected MTC mutants were pregrown on YNBcas, transferred as suspensions onto YPD (A), YNBcas (B), YNBD (C), YNBO (D), and YNBT (E) plates, and incubated at 28°C for 2 to 5 days. Mutants and their phenotypes: auxotrophic mutant N083 (Aux, later shown to be *leu1* [Fig. 7]); morphology mutants N005 (Fil^{++} [very rough hyperfilamentous colonies] Alk^+ Faa^+ Tbu^+ Lip^- [no halo formation due to extracellular lipase activity] Glu^+), N203 (Fil^- [smooth colonies, only yeast form] Alk^+ Faa^+ Tbu^+ Lip^- Glu^+), and N127 (Spr^+ [spreading and filamenting] Alk^+ Faa^+ Tbu^+ Lip^+ Glu^+); and HC degradation mutants N006 (alkD/E: Alk^- [C_{10}^- C_{12}^- C_{16}^-] Faa^- Tbu^+ Lip^+ [normal halo formation] $Eth^{+/-}$ Glu^+ Fil^-), N046 (alkAc: Alk^- C_{16} [C_{10}^+ $C_{12}^{+/-}$ $C16^-$] Faa^+ Tbu^+ Lip^+ Glu^+ Fil^- [Fig. 6]), N059 (Alk^- [growth delay] [$C_{10}^{+/-}$ $C_{12}^{+/-}$ $C_{16}^{+/-}$] Faa^+ Tbu^+ Lip^+ Glu^+), N137 (Lip^{++} [large halo formation on YNBT] Alk^+), N216 (alkE: all HC^- Alk^- [C_{10}^- C_{12}^- C_{16}^-] Faa^- Tbu^- Eth^- Glu^+ Fil^-), N221 ($Alk^{+/-}$ $Faa^{+/-}$ Tbu^+ Lip^- [no halo] Glu^+ $Fil^{+/-}$), and N240 (alkAb: Alk^- C_{10} [C_{10}^- $C_{12}^{+/-}$ $C_{16}^{+/-}$] Faa^+ Tbu^+ Lip^+ Glu^+).

expected profile after MTC integration was observed in most of the transformants, resulting in five bands (type II), as predicted above (the two smallest bands, bands b and b′, comigrate and show doubled intensity [Fig. 4B and C]). This type II pattern was observed in 13 out of 20 T clones (65%) (Fig. 4B) and in 18 out of 21 P clones (86%) (Fig. 4C). Nonexpected patterns suggesting multiple insertion of the MTC (more than five bands and higher intensity of band d, type III) were observed for four T clones (Fig. 4B, clones 3, 19, and probably 5 and 14) and for three P clones (Fig. 4C, clones 1, 10, and 13). This indicates that most events resulted from single MTC integration at different loci.

Phenotypic analysis of tagged mutants. To assess the efficiency of MTC for isolating mutants affected in HC utilization, we screened approximately 8,600 Ura^+ transformants for their ability to grow on nine media, including HC (alkanes, fatty acid, and triglyceride), ethanol, and glucose, and on media inducing hyphal growth. Transformants were first transferred onto YNBcas and then replica plated to avoid colony size effects. YPD, YNBcas, and YNBG were used for morphology and auxotrophy testing. An amino acid-auxotrophic strain such as N083 (Fig. 5) will grow only on YPD and YNBcas. HC utilization was analyzed on *n*-alkanes of different chain lengths (YNBC10, YNBC12, or YNBC16), oleic acid (YNBO), and tributyrin (YNBT) and compared to the growth on the hydrophilic substrates ethanol (YNBE) and glucose (YNBD). The YNBT medium also revealed halo formation due to extracellular lipase or esterase production.

Thus, 257 mutants were isolated out of 8,600 transformants, purified, and retested on the same media in 96-well microtiter plates as described previously (18). Clear phenotypes were confirmed for about 170 of these primary clones. This mutant frequency of 2% is close to the 2.5% frequency previously obtained with Tn*3* insertion (18). Selected mutants were subsequently tested in liquid cultures. Examples of mutant phenotypes are shown in Fig. 5 and 6.

About 70 mutants were affected with regard to growth on at least one of the three types of hydrophobic substrates (alkanes [Alk^-], the fatty acid oleate [Faa^-], and the triglyceride tributyrin [Tbu^-]). Other carbon source utilization phenotypes, such as no growth on ethanol only (Alk^+ Eth^- Glu^+, similar to N004), and four yellowish or brownish mutants were also obtained. Other less clear phenotypes, such as reduced growth on glucose, which are not easily distinguished from leaky auxotrophy were eliminated.

Among these HC^- mutants, about 45 exhibited a phenotype involved in the utilization of alkanes and fatty acid, such as alkA (Alk^- Faa^+ Eth^+ Glu^+), alkD (Alk^- Faa^- Eth^+ Glu^+), and alkE (Alk^- Faa^- Eth^+ Glu^+). Examples of these mutants are shown in Fig. 5 and 6. The alkD clones N002 (Fig. 6) and N040 (data not shown) did not grow on any alkane or on oleic acid but did grow on ethanol and glucose and showed a smooth (Fil^-) colony morphology. The alkE clones N216 (Fig. 5), N078, and N156 (data not shown) did not grow on any alkane, on fatty acid, or on ethanol but did grow on glucose and also showed a smooth (Fil^-) colony morphology. The alkA (Alk^- Faa^+) mutants exhibited growth defects depending on alkane chain length. They either did not grow on any alkane (alkAa [C_{10}^- C_{12}^- C_{16}^-]), like N029 (data not shown), or exhibited chain length preferences; for example, N032 grew with a lag on C_{10} but well on C_{16} (alkAb), whereas N046 grew on C_{10} but not on C_{16} (alkAc) (Fig. 6), representing the first stable alkAc *Y. lipolytica* mutants isolated. Other Alk mutants appeared to be leaky (delayed growth on alkanes) or unstable after replica plating or in drop tests (not shown), indicating frequent occurrence of spontaneous suppressor mutations.

Several Alk^- and Faa^- mutants were also affected in tributyrin utilization (Tbu^-), although this was not the case for all Alk^- mutants, like N006 (Alk^- Faa^- Tbu^+ Lip^+ Glu^+) (Fig. 5). On YNBT medium, 36 mutants appeared to be affected with regard to extracellular lipase activities, as observed by halo formation. Besides normal halo formation (Lip^+, wild-type) observed for several mutants showing other phenotypes, we observed both Lip^- phenotypes (no halo formation at all, as for N047, N203, and N221) and Lip^{++} phenotypes (larger halo, like N137, N185, N235, and N256) (Fig. 5D).

In the primary screening, about 50 auxotrophic mutants were obtained. Strain N083 was found to be auxotrophic for leucine and shown to be interrupted in the *LEU1* gene (see below).

We also observed about 90 mutants with morphologies that were abnormal compared to that of the wild-type strain. Although colonial morphology varied on different media, about

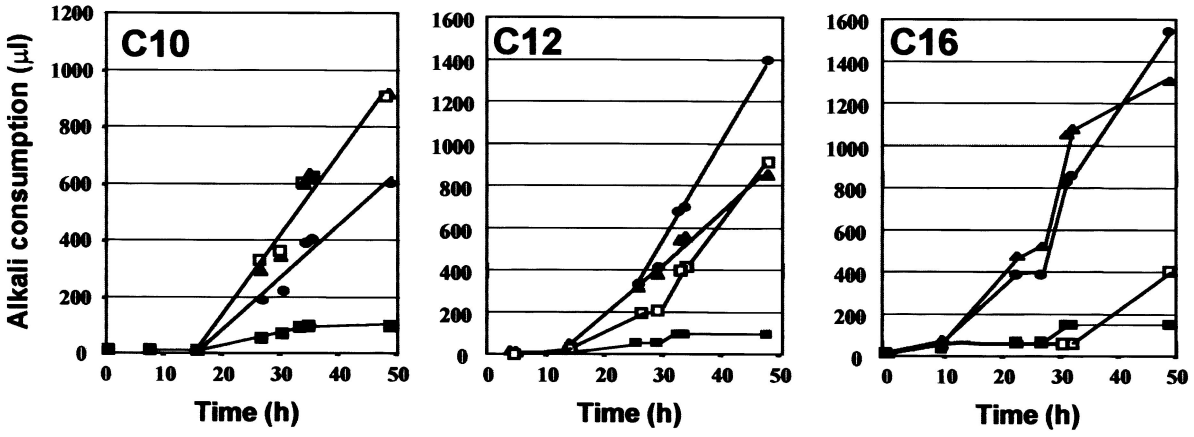

FIG. 6. Growth of selected Alk$^-$ mutants on alkanes of different chain lengths. Growth of the insertion mutant was tested in shaking flasks with 1% alkane medium (YNBC10, YNBC12, or YNBC16). ■, N002 (alkD: Alk$^-$ [$C_{10}{}^-$ $C_{12}{}^-$ $C_{16}{}^-$] Faa$^-$ Tbu$^+$ Eth$^+$ Glu$^+$ Fil$^-$); ●, N032 (alkAb or alkA leaky: Alk$^{+/-}$ [$C_{10}{}^{+/-}$ $C_{12}{}^{+/-}$ $C_{16}{}^+$] Faa$^+$ Tbu$^+$ Eth$^+$ Glu$^+$); □, N046 (alkAc: Alk$^-$ C_{16} [$C_{10}{}^+$ $C_{12}{}^{+/-}$ $C_{16}{}^-$] Faa$^+$ Tbu$^+$ Glu$^+$ Fil$^-$); ▲, N233 (alkA leaky: Alk$^{+/-}$ [$C_{10}{}^+$ $C_{12}{}^{+/-}$ $C_{16}{}^+$] Faa$^+$ Eth$^+$ Glu$^+$). Mutants were cultivated, and growth was monitored as for Fig. 3.

25 mutants were hyperfilamentous on various media (Fil^{++}, like N005), a phenotype not reported previously. A majority of mutants produced smooth, yeast-cell-only-containing colonies (Fil$^-$, like N002, N006, and N203), and eight mutants with larger and flat colonies were called spreading (Spr$^+$, like N127). Some examples of these phenotypes are shown in Fig. 5. Interestingly, most Fil$^-$ mutants were also affected in alkane and fatty acid utilization, presenting mostly an alkD or alkE phenotype, like N002, N006, or N216. They might be due to MTC insertion in a *PEX* gene, since mutants affected in both morphology and fatty acid utilization were previously described as being affected in peroxisome biogenesis (32), like mutant JMY226 (18), in which *PEX10* is interrupted.

These results show that MTC is highly efficient for the induction of mutants affected in different pathways and can be used for creating various mutant libraries in *Y. lipolytica.*

Analysis of the insertion event and identification of the interrupted gene. To analyze the insertion event and identify the interrupted gene in tagged mutants, the MTC borders were amplified by either divergent or convergent PCR (26, 31) (Fig. 2) as described in Materials and Methods.

Results for the leucine-auxotrophic mutant N083 are presented in Fig. 7. Borders of the MTC were amplified by PCR walking and sequenced with the specific MTC primers Zeta1 and Zeta3 and with the adapter-specific primer Ap1. BLAST analysis revealed sequences similar to part of the *LEU1* gene, encoding 3-isopropylmalate dehydratase, of *Saccharomyces cerevisiae* (YGL009c). Within the Zeta1 and Zeta3 sequences (Fig. 7B, lines 3 and 5, respectively), the left and right parts of the MTC sequences (Fig. 7B, lines 4 and 6, respectively) were followed by *LEU1* sequences (Fig. 7B, line 2). To identify the genomic sequence at the insertion site, part of the *LEU1* gene was amplified with primer pair N083-1–N083-2 using H222-41 DNA as the template, and the PCR fragment was sequenced. Comparison of the genomic DNA sequence with the left and right border sequences revealed that the MTC was partially degraded (deletion of 2 and 14 bp from the left and right ends, respectively) (Table 2). Additionally, no sequence similar to the *Not*I site could be observed at the insertion site, indicating that insertion was not site specific or mediated by a restriction enzyme-mediated integration-type mechanism into *Not*I-like GC rich regions (28) and that MTC integrates by nonhomologous recombination.

A similar approach was used for 64 MTC insertion mutants. Results are presented in Table 2 for clones N156, N216, N222, and N225. For the last three clones, RSTs from *Y. lipolytica* (8)

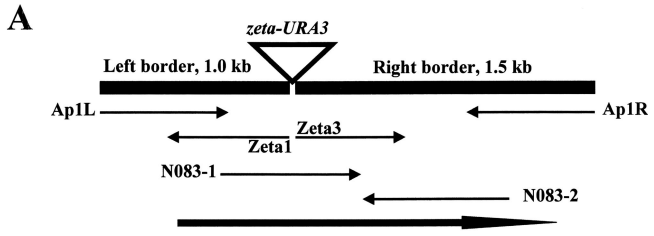

B

```
1 GluAlaArgMetSerMetCysAsnMetAlaIleGluGlyGlyAla
2 GAGGCTCGAATGTCCATGTGCAACATGGCGATTGAGGGAGGAGCT
3 GAGGCTCGAATGTCCATGccgcctgtgggg
4             ggccgcctgtgggg
5       tctcacaaagccctCAACATGGCGATTGAGGGAGGAGCT
6       tctcacaaagcccttcagtgtgcggcc
```

FIG. 7. Sequencing of the insertion site in mutant N083. (A) Schematic representation of the *zeta-URA3* MTC insertion in mutant N083. The amplified border fragments obtained by convergent PCR (black boxes; PCR walking as described in reference 9) and the sequence determined (arrows) using the MTC-specific primers Zeta1 and Zeta3, the adapter-specific primer Ap1 for the left (Ap1L) and the right (Ap1R) border fragments, and the gene-specific primers N083-1 and N083-2 are shown. The bold arrow indicates the location of the *LEU1* gene (AJ278693). (B) Partial amino acid (line 1) and corresponding nucleic (line 2) sequences of the wild-type *LEU1* gene (amplified with the primers N083-1 and N083-1 from the genomic locus) and the sequences obtained with Zeta1 (line 3) and Zeta3 (line 5), compared with the left (line 4) and right (line 6) borders of the *Not*I *zeta-URA3* cassette (in lowercase letters). The underlined lowercase letters correspond to the *Not*I site of the cassette borders (lines 4 and 6). The sequence underlined in line 2 corresponds to the 2-bp deletion at the site of MTC insertion into the *LEU1* gene.

TABLE 2. MTC insertion characteristics

Mutant	Sequence origin	Deletion size (bp)[a]		Size (kb) of amplified fragment[b]	
		Left	Right	Left	Right
N083	PCR fragment	2	14	0.9	1.6
N156	PCR fragment	2	0	0.5	1.5
N216	AWOAA019F02T1[c]	6	13	0.7	0.8
N222	AWOAA012C01D1[c]	7	0	1.4	1.2
N225	AWOAA017A04D1[c]	—[d]	1	1.1	1.7

[a] Deletion observed on both sides of the MTC after insertion.
[b] The left and right borders were amplified by the convergent method using Ap1-Zeta 1 and Ap1-Zeta3 primer pairs, respectively.
[c] RSTs overlapping the insertion site, from reference 8.
[d] Addition of 50 bp.

overlap the two borders, allowing identification of the wild-type sequence at the insertion site of the MTC. This comparison shows that MTC ends were trimmed over a few base pairs on both sides and integrated by nonhomologous recombination with a few base pairs modified at the insertion site.

A total of 64 mutants were tested to determine the MTC insertion site by convergent PCR amplification after *Eco*RV restriction and PCR walking (Fig. 2). Both borders were obtained for 32 clones, one border was obtained only for 25 clones, and none was obtained for 7 clones. A new PCR walking was performed with genomic DNA digested by three restriction enzymes, *Eco*RV, *Stu*I, and *Pvu*II. This increased the number of borders that could be amplified. However, the sizes of the amplified fragments were smaller, decreasing the number of significant BLAST results (data not shown).

For 15 clones, sequence analysis revealed atypical integration events. We obtained seven clones with the insertion of two MTCs either head to tail, head to head, or tail to tail. For example, in the alkD mutant N002 (Alk^- Faa^- Eth^+ Glu^+), two copies of the MTC integrated in tandem and in the same orientation. For five clones, we observed integration of JMP5, resulting from a single *Not*I digestion of the vector. For three clones, we observed the insertion of one MTC flanked by two copies of the vectors or insertion of the vector flanked by two MTCs. These events probably reflect partial digestion of JMP5 and/or in vivo ligation of the MTCs prior integration.

To identify the disrupted genes, we sequenced the borders of the MTC using the PCR walking method as shown above for N083 (Fig. 7). Sequence analysis revealed that the insertion occurred in the isocitrate dehydrogenase gene for mutant N156 (alkE leaky: Alk^- Faa^- $Eth^{+/-}$ Glu^+), in the thioredoxin reductase gene for N040 (alkD: Alk^- Faa^- Eth^- Glu^+ Fil^- and yellowish), and in the peroxine 14 gene (*PEX14* [unpublished data]) for mutant N078 (alkD: Alk^- Faa^- Eth^- Glu^+ Fil^-). A thorough analysis of the disrupted genes will be presented elsewhere.

Taken together, these results demonstrate that amplification and sequencing of the MTC insertion sites permit efficient and unambiguous identification of the interrupted genes and suggest that this method should be generally useful to identify genes in any pathway.

ACKNOWLEDGMENTS

This work was supported by the Institut National de la Recherche Agronomique and by the Centre National de la Recherche Scientifique (France), and it benefited from the France-Germany exchange program PROCOPE for 1998–2000 (MAE—A.P.A.P.E. no. 98185; DAAD PKZ 9723054).

The technical assistance of Susann Berthold is gratefully acknowledged. We thank Claudia Rentsch for the construction of plasmid pCR4, Fanny Aubertin for participation in mutant screening, and Antje Augstein for sharing results on the presence of *Ylt1* in different *Y. lipolytica* strains.

REFERENCES

1. **Altschul, S. F., T. L. Madden, A. A. Schaffer, J. Zhang, Z. Zhang, W. Miller, and D. J. Lipman.** 1997. Gapped BLAST and PSI-BLAST: a new generation of protein database search programs. Nucleic Acids Res. **25:**3389–3402.
2. **Barth, G., and C. Gaillardin.** 1997. Physiology and genetics of the dimorphic fungus *Yarrowia lipolytica*. FEMS Microbiol. Rev. **19:**219–237.
3. **Barth, G., and C. Gaillardin.** 1996. *Yarrowia lipolytica*, p. 313–388. *In* K. Wolf (ed.), Nonconventional yeasts in biotechnology. Springer-Verlag, Berlin, Germany.
4. **Barth, G., and T. Scheuber.** 1993. Cloning of the isocitrate lyase gene (*ICL1*) from *Yarrowia lipolytica* and characterization of the deduced protein. Mol. Gen. Genet. **241:**422–430.
5. **Bassel, J. B., and R. K. Mortimer.** 1982. Genetic and biochemical studies of n-alkane non-utilizing mutants of *Saccharomycopsis lipolytica*. Curr. Genet. **5:**77–88.
6. **Bassel, J. B., and R. K. Mortimer.** 1985. Identification of mutations preventing n-hexadecane uptake among 26 n-alkane non-utilizing mutants of *Yarrowia lipolytica*. Curr. Genet. **9:**579–586.
7. **Casaregola, S., C. Feynerol, M. Diez, P. Fournier, and C. Gaillardin.** 1997. Genomic organization of the yeast *Yarrowia lipolytica*. Chromosoma **106:** 380–390.
8. **Casaregola, S., C. Neuveglise, A. Lepingle, E. Bon, C. Feynerol, F. Artiguenave, P. Wincker, and C. Gaillardin.** 2000. Genomic exploration of the hemiascomycetous yeasts: 17. *Yarrowia lipolytica*. FEBS Lett. **487:**95–100.

8a. **Davidow, L. S., and J. R. Dezeeuw.** 10 May 1983. Process for transforming Yarrowia lipolytica. U.S. patent US539591.

9. **Devic, M., S. Albert, M. Delseny, and T. Roscoe.** 1997. Efficient PCR walking on plant genomic DNA. Plant Physiol. Biochem. **35:**331–339.
10. **Huth, J., S. Werner, and H.-G. Müller.** 1990. The proton extrusion of growing yeast cultures as an on-line parameter in fermentation processes: quantitative determination of growth from milligram amounts of substrate in a minimized fed-batch fermentation apparatus. J. Basic Microbiol. **7:**489–497.
11. **Iida, T., A. Ohta, and M. Takagi.** 1998. Cloning and characterization of an n-alkane-inducible cytochrome P450 gene essential for n-decane assimilation by *Yarrowia lipolytica*. Yeast **14:**1387–1397.
12. **Iida, T., T. Sumita, A. Ohta, and M. Takagi.** 2000. The cytochrome P450ALK multigene family of an n-alkane-assimilating yeast, *Yarrowia lipolytica*: cloning and characterization of genes coding for new *CYP52* family members.Yeast **16:**1077–1087.
13. **Juretzek, T., M. T. Le Dall, S. Mauersberger, C. Gaillardin, G. Barth, and J.-M. Nicaud.** 2001. Vectors for gene expression and amplification in the yeast *Yarrowia lipolytica*. Yeast **18:**97–113.
14. **Kujau, M., H. Weber, and G. Barth.** 1992. Characterization of mutants of the yeast *Yarrowia lipolytica* defective in acetyl-coenzyme A synthetase. Yeast **8:**193–203.
15. **Lindley, N. D.** 1995. Bioconversion and biodegradation of aliphatic hydrocarbons. Can. J. Bot. **73**(Suppl. 1)**:**S1034–S1042.
16. **Mauersberger, S.** 1991. Mutants of alkane oxidation in the yeasts *Yarrowia lipolytica* and *Candida maltosa*, p. 59–78. *In* A. A. Sharyshev and T. V. Finogenova (ed.), Alkane metabolism and oversynthesis of metabolites by microorganisms. Center for Biological Research, USSR Academy of Sciences, Pushchino, USSR.
17. **Mauersberger, S., M. Ohkuma, W.-H. Schunck, and M. Takagi.** 1996. *Candida maltosa*, p. 411–580. *In* K. Wolf (ed.), Nonconventional yeasts in biotechnology. Springer-Verlag, Berlin, Germany.
18. **Neuveglise, C., J.-M. Nicaud, P. Ross-Macdonald, and C. Gaillardin.** 1998. A shuttle mutagenesis system for tagging genes in the yeast *Yarrowia lipolytica*. Gene **213:**37–46.
19. **Nga, B. H., C. M. Gaillardin, P. Fournier, and H. Heslot.** 1989. Genetic analysis of lipase low-producing mutants of *Yarrowia lipolytica*. J. Gen. Microbiol. **135:**2439–2444.
20. **Nga, B. H., H. Heslot, C. M. Gaillardin, P. Fournier, K. Chan, Y. N. Chan, E. W. Lim, and P. C. Nai.** 1988. Use of nystatin for selection of tributyrin non-utilizing mutants in *Yarrowia lipolytica*. J. Biotechnol. **7:**83–86.
21. **Nicaud, J.-M., E. Fabre, and C. Gaillardin.** 1989. Expression of invertase activity in *Yarrowia lipolytica* and its use as a selective marker. Curr. Genet. **16:**253–260.
22. **Nuttley, W. M., A. M. Brade, C. Gaillardin, G. A. Eitzen, J. R. Glover, J. D.**

Aitchison, and R. A. Rachubinski. 1993. Rapid identification and characterization of peroxisomal assembly mutants in *Yarrowia lipolytica*. Yeast **9:**507–517.
23. **Ohkuma, M., T. Zimmer, T. Iida, W.-H. Schunck, A. Ohta, and M. Takagi.** 1998. Isozyme function of n-alkane-inducible cytochromes P450 in *Candida maltosa* revealed by sequential gene disruption. J. Biol. Chem. **273:**3948–3953.
24. **Pignède, G., H. J. Wang, F. Fudalej, C. Gaillardin, M. Seman, and J.-M. Nicaud.** 2000. Characterization of an extracellular lipase encoded by *LIP2* in *Yarrowia lipolytica*. J. Bacteriol. **182:**2802–2810.
25. **Pignède, G., H.-J. Wang, F. Fudalej, M. Seman, C. Gaillardin, and J.-M. Nicaud.** 2000. Autocloning and amplification of *LIP2* in *Yarrowia lipolytica*. Appl. Environ. Microbiol. **66:**3283–3289.
26. **Richard, M., R. Quijano, S. Bezzate, F. Bordon-Pallier, and C. Gaillardin.** 2001. Tagging morphogenetic genes by insertional mutagenesis in the yeast *Yarrowia lipolytica*. J. Bacteriol. **183:**3098–3107.
27. **Sambrook, J., T. Maniatis, and E. F. Fritsch.** 1989. Molecular cloning: a laboratory manual, 2nd ed. Cold Spring Harbor Laboratory Press, Cold Spring Harbor, N.Y.
28. **Sanchez, O., R. E. Navarro, and J. Aguirre.** 1998. Increased transformation frequency and tagging of developmental genes in *Aspergillus nidulans* by restriction enzyme-mediated integration (REMI). Mol. Gen. Genet. **258:**89–94.
29. **Schmid-Berger, N., B. Schmid, and G. Barth.** 1994. *Ylt1*, a highly repetitive retrotransposon in the genome of the dimorphic fungus *Yarrowia lipolytica*. J. Bacteriol. **176:**2477–2482.
30. **Shennan, J. L., and J. D. Levi.** 1974. The growth of yeast on hydrocarbons. Prog. Ind. Microbiol. 13:1–57.
31. **Siebert, P., A. Chenchik, D. Kellogg, K. Lukyanov, and S. Lukyanov.** 1995. An improved PCR method for walking in uncloned genomic DNA. Nucleic Acids Res. **23:**1087–1088.
32. **Titorenko, V. I., D. M. Ogrydziak, and R. A. Rachubinski.** 1997. Four distinct secretory pathways serve protein secretion, cell surface growth, and peroxisome biogenesis in the yeast *Yarrowia lipolytica*. Mol. Cell. Biol. **17:**5210–5226.
33. **Titorenko, V. I., and R. A. Rachubinski.** 2001. Dynamics of peroxisome assembly and function. Trends Cell Biol. **11:**22–29.
34. **Tzschoppe, K., A. Augstein, R. Bauer, S. D. Kohlwein, and G. Barth.** 1999. Trans-dominant mutations in the *GPR1* gene cause high sensitivity to acetic acid and ethanol in the yeast *Yarrowia lipolytica*. Yeast **15:**1645–1656.
35. **Wang, H. J., M.-T. Le Dall, Y. Wach, C. Laroche, J. M. Belin, C. Gaillardin, and J. M. Nicaud.** 1999. Evaluation of acyl coenzyme A oxidase (Aox) isozyme function in the *n*-alkane-assimilating yeast *Yarrowia lipolytica*. J. Bacteriol. **181:**5140–5148.
36. **Wolf, K. (ed.).** 1996. Nonconventional yeasts in biotechnology. Springer Verlag, Berlin, Germany.
37. **Zimmer, T., T. Iida, W.-H. Schunck, Y. Yoshida, A. Ohta, and M. Takagi.** 1998. Relation between evolutionary distance and enzymatic properties among the members of the *CYP52A* subfamily of *Candida maltosa*. Biochem. Biophys. Res. Commun. **251:**244–247.